World Journal of Diabetes

Submit a Manuscript: https://www.f6publishing.com

World J Diabetes 2024 July 15; 15(7): 1537-1550

DOI: 10.4239/wjd.v15.i7.1537

ISSN 1948-9358 (online)

ORIGINAL ARTICLE

Observational Study

Glymphatic function and its influencing factors in different glucose metabolism states

Bin Tian, Chen Zhao, Jia-Li Liang, Hui-Ting Zhang, Yi-Fan Xu, Hui-Lei Zheng, Jia Zhou, Jiang-Nian Gong, Shu-Ting Lu, Zi-San Zeng

Specialty type: Endocrinology and metabolism

Provenance and peer review: Unsolicited article; Externally peer reviewed.

Peer-review model: Single blind

Peer-review report's classification

Scientific Quality: Grade B; Grade C

Novelty: Grade C

Creativity or Innovation: Grade C

Scientific Significance: Grade C

P-Reviewer: Cigrovski Berkovic M, Croatia; Ghusn W, United States

Received: February 26, 2024

Revised: May 13, 2024

Accepted: June 11, 2024

Published online: July 15, 2024

Processing time: 132 Days and 20.8 Hours

Bin Tian, Jia-Li Liang, Yi-Fan Xu, Jiang-Nian Gong, Shu-Ting Lu, Zi-San Zeng, Department of Radiology, The First Affiliated Hospital of Guangxi Medical University, Nanning 530021, Guangxi Zhuang Autonomous Region, China

Chen Zhao, Magnetic Resonance Research Collaboration, Siemens Healthineers, Guangzhou 510620, Guangdong Province, China

Hui-Ting Zhang, Magnetic Resonance Research Collaboration, Siemens Healthineers Ltd., Wuhan 430071, Hubei Province, China

Hui-Lei Zheng, Department of Health Management, The First Affiliated Hospital of Guangxi Medical University, Nanning 530021, Guangxi Zhuang Autonomous Region, China

Jia Zhou, Department of Endocrinology, The First Affiliated Hospital of Guangxi Medical University, Nanning 530021, Guangxi Zhuang Autonomous Region, China

Corresponding author: Zi-San Zeng, MD, Chief Doctor, Professor, Department of Radiology, The First Affiliated Hospital of Guangxi Medical University, No. 6 Shuangyong Road, Nanning 530021, Guangxi Zhuang Autonomous Region, China. zengzisan@aliyun.com

Abstract

BACKGROUND

Dysfunction of the glymphatic system in the brain in different stages of altered glucose metabolism and its influencing factors are not well characterized.

AIM

To investigate the function of the glymphatic system and its clinical correlates in patients with different glucose metabolism states, the present study employed diffusion tensor imaging along the perivascular space (DTI-ALPS) index.

METHODS

Sample size was calculated using the pwr package in R software. This cross-sectional study enrolled 22 patients with normal glucose metabolism (NGM), 20 patients with prediabetes, and 22 patients with type 2 diabetes mellitus (T2DM). A 3.0T magnetic resonance imaging was used to evaluate the function of the glymphatic system. The mini-mental state examination (MMSE) was used to assess general cognitive function. The DTI-ALPS index of bilateral basal ganglia

and the mean DTI-ALPS index was calculated. Further, the correlation between DTI-ALPS and clinical features was assessed.

RESULTS

The left-side, right-side, and mean DTI-ALPS index in the T2DM group were significantly lower than that in the NGM group. The right-side DTI-ALPS and mean DTI-ALPS index in the T2DM group were significantly lower than those in the prediabetes group. DTI-ALPS index lateralization was not observed. The MMSE score in the T2DM group was significantly lower than that in the NGM and prediabetes group. After controlling for sex, the left-side DTI-ALPS and mean DTI-ALPS index in the prediabetes group were positively correlated with 2-hour postprandial blood glucose level; the left-side DTI-ALPS index was negatively correlated with total cholesterol and low-density lipoprotein level. The right-side DTI-ALPS and mean DTI-ALPS index were negatively correlated with the glycosylated hemoglobin level and waist-to-hip ratio in the prediabetes group. The left-side, right-side, and mean DTI-ALPS index in the T2DM group were positively correlated with height. The left-side and mean DTI-ALPS index in the T2DM group were negatively correlated with high-density lipoprotein levels.

CONCLUSION

Cerebral glymphatic system dysfunction may mainly occur in the T2DM stage. Various clinical variables were found to affect the DTI-ALPS index in different glucose metabolism states. This study enhances our understanding of the pathophysiology of diabetic brain damage and provides some potential biological evidence for its early diagnosis.

Key Words: Glymphatic system; Prediabetes; Type 2 diabetes mellitus; Magnetic resonance imaging; Diffusion tensor imaging along the perivascular space

Core Tip: Dysfunction of the glymphatic system in the brain in different stages of altered glucose metabolism is not well characterized. This study employed diffusion tensor imaging along the perivascular space (DTI-ALPS) index to investigate the function of the glymphatic system and its clinical correlates in patients with different glucose metabolism states. Cerebral glymphatic system dysfunction was found to mainly occur in overt diabetes mellitus. Various clinical variables were found to affect the DTI-ALPS index in different stages of impaired glucose metabolism.

Citation: Tian B, Zhao C, Liang JL, Zhang HT, Xu YF, Zheng HL, Zhou J, Gong JN, Lu ST, Zeng ZS. Glymphatic function and its influencing factors in different glucose metabolism states. *World J Diabetes* 2024; 15(7): 1537-1550
URL: https://www.wjgnet.com/1948-9358/full/v15/i7/1537.htm
DOI: https://dx.doi.org/10.4239/wjd.v15.i7.1537

INTRODUCTION

The progressive population aging and unhealthy lifestyles have contributed to the increase in the prevalence of prediabetes and diabetes. Currently, an estimated 415 million individuals are diagnosed with diabetes, and an additional 31.8 billion people are considered to be prediabetic[1]. Prediabetes and type 2 diabetes mellitus (T2DM) account for approximately 90% of all diabetes diagnoses. Prolonged hyperglycemia can cause microvascular (such as endothelial, pericyte, and vascular smooth muscle cell injury) and macrovascular injury[2,3], resulting in disabling complications, including retinopathy, nephropathy, neuropathy, cardiovascular disease, and cerebrovascular disease[1,4]. Simultaneously, over 47 million individuals are currently affected by dementia, and this figure is projected to triple by the year 2050[5]. Numerous population-based studies have demonstrated that individuals with diabetes or prediabetes are at an increased risk of developing Alzheimer's disease (AD)[6] and faster deterioration of cognitive function[7].

The glymphatic system is a perivascular network in the brain for the exchange of cerebrospinal fluid (CSF) and interstitial fluid (ISF)[8,9]. Impairment of the glymphatic system is suggested to be associated with reduced cognitive function[10,11]. This system encompasses three primary structures, namely the periarterial CSF inflow channel, the ravenous ISF outflow channel, and the astrocyte exchange channel (aquaporin-4, AQP4), which serves as the connecting link between the aforementioned channels[12]. The glymphatic system plays a crucial role in the elimination of metabolic waste products from the brain[13], including amyloid β protein (Aβ) and metabolites, as well as the distribution of glucose, lipids, amino acids, and neuromodulators[14,15]. In addition, this system is closely related to the pathophysiology of various neurological diseases, such as Parkinson's disease (PD)[16,17] and AD[18]. Studies have demonstrated the involvement of the glymphatic dysfunction in the pathophysiology of diabetic brain injury[19]. We believe that glymphatic dysfunction is likely associated with brain injury pathology in different stages of impaired glucose metabolism. Evaluating the potential association between the brain's lymphatic function in different glucose

metabolism states and alterations in white matter microstructure can help characterize the involvement of the glymphatic system in the pathophysiological changes in different stages of impaired glucose metabolism.

The glymphatic system has been investigated through *ex vivo* fluorescence microscopy and *in vivo* two-photon imaging in animal models[14,20] as well as in humans using intrathecal contrast-enhanced magnetic resonance imaging (MRI)[21] and dynamic positron emission tomography[22]. However, the invasiveness of these methods and their associated risks restrict their application in human studies. Therefore, it is imperative to develop an enhanced, noninvasive technique for a reliable assessment of glymphatic system function.

Recent advances in MRI techniques, particularly diffusion tensor imaging (DTI), have facilitated the functional evaluation of the glymphatic system. However, structural modifications can potentially impact the DTI-derived characteristics within the glymphatic system. Recently, a noninvasive approach called DTI-ALPS has been developed for the functional assessment of the glymphatic system within the brain[11]. This method involves generating water diffusivity measurements along the x, y, and z axes of the periventricular space (PVS) white matter using a diffusion sequence, which is then utilized to calculate the DTI-analysis method along the perivascular space (ALPS) index.

The DTI-ALPS index is used to measure water diffusivity along the x-axis, which aligns with the direction of the PVS and can indicate the function of the glymphatic system[11,16]. This methodology has been employed for investigating various neurological conditions, such as diabetes mellitus (DM)[19], AD[23], PD[24-26], rapid eye movement sleep behavior disorder[27], epilepsy[28], and idiopathic normal pressure hydrocephalus[29]. These studies suggest that the DTI-ALPS index can be used as a noninvasive imaging biomarker for assessing glymphatic system function.

Hence, the objective of this study was to employ the DTI-ALPS index for assessing the functionality of the glymphatic system in individuals with different glucose metabolism states. Additionally, we aimed to investigate the specific stage at which dysfunction of the glymphatic system occurs and explore the factors influencing the DTI-ALPS index for early diagnosis and further understanding the pathophysiological mechanism of diabetic brain injury to explore new evidence. We evaluated these indicators to substantiate the hypothesis of diminished perivascular fluid diffusion and impairment of perivascular structures in patients with different stages of impaired glucose metabolism. To investigate the determinants of the DTI-ALPS index, we conducted additional analysis to examine the association between the DTI-ALPS index and clinical characteristics. Our findings may help identify novel biomarkers and factors influencing glymphatic system damage under different glucose metabolic states. This study may enhance our understanding of the pathophysiology of diabetic brain injury and provide new evidence for its early diagnosis.

MATERIALS AND METHODS

Participants and clinical data collection

This study was approved by the ethics committee of The First Affiliated Hospital of Guangxi Medical University (approval No. 2023-K118-01) and has been registered in the Chinese Clinical Trials Registry (registration No. ChiCTR2300075515).

The power analyses were conducted using the pwr package in R software, factoring a significance level of $P = 0.05$, a target power of 0.8, and an effect size was of $r = 0.4$[30,31]. The power analysis for the analysis of variance indicated a minimum sample size of 64 participants to achieve a power of 80%. In this study, 64 participants who qualified the inclusion criteria were recruited, including 22 with normal glucose metabolism (NGM) as controls, 20 with prediabetes, and 22 with T2DM. The three groups were matched for sex and age. The inclusion criteria were: (1) Right-handed; (2) Number of years of education: ≥ 6; (3) No history of thyroid, heart, liver, or kidney diseases; (4) No history of neurological or psychiatric diseases such as PD and epilepsy; (5) No history of brain diseases (tumor, hemorrhage, infarction) or traumatic brain injury; and (6) No contraindications to MRI.

Each subject provided a medical history and underwent a physical examination, during which clinical data were recorded or measured by standard laboratory tests. These variables included sex, age, years of education, height, weight, body mass index (BMI), waist circumference, hip circumference, waist-to-hip ratio, fasting plasma glucose (FPG), 2-hour postprandial blood glucose (2hPG), glycosylated hemoglobin (HbA1c), fasting insulin (FINS), blood pressure, total cholesterol (TC), triglycerides, high-density lipoprotein (HDL), and low-density lipoprotein (LDL). Educational level was recorded in terms of years of education: Six years for elementary school graduation, nine years for junior high school graduation, twelve years for high school graduation or vocational high school, fifteen years for college students, sixteen years for bachelor's degree, nineteen years for master's degree, and twenty-two years for doctoral degree. BMI was calculated as BMI = weight (kg)/[height (m)]^2. Insulin resistance score was determined using insulin resistance index (HOMA-IR), which was calculated as follows: HOMA-IR = (FPG, mmol/L) × (FINS, pmol/L)/135. Normal individuals have a HOMA-IR index of 1, which may be higher than 1 as the level of insulin resistance increases.

Since the DM diagnosis and the glucose metabolism status classification were based on the 1999 World Health Organization diagnostic criteria, plasma glucose analysis was conducted only at two time points of FPG and 2hPG. The subjects were divided according to the status of glucose metabolism and the history of DM: (1) T2DM was diagnosed using established criteria based on medical history, medication use, FPG ≥ 7.0 mmol/L and 2hPG ≥ 11.1, the first diagnosis of T2DM; (2) Prediabetes group: Impaired fasting glucose (6.1 mmol/L ≤ FPG < 7.0 mmol/L and 2hPG < 7.8 mmol/L) and impaired glucose tolerance (FPG < 7.0 mmol/L and 7.8 mmol/L ≤ 2hPG < 11.1 mmol/L); (3) FPG < 6.1 mmol/L and 2hPG < 7.8 mmol/L.

The mini-mental state examination (MMSE) was used to evaluate the overall cognitive function; the MMSE score ranged from 0 to 30 points.

Magnetic resonance image acquisition

A 3.0T MRI scanner (MAGNETOM Prisma, Siemens Healthineers, Germany) with a 64-channel combined head and neck coil was used for the imaging of all volunteers. Conventional magnetic resonance sequences, including T1-weighted imaging, T2-weighted imaging, T2-fluid attenuated inversion recovery, and diffusion-weighted imaging (DWI), were employed to detect and characterize brain tumors, cerebral hemorrhage, and cerebral infarction. Diffusion spectrum imaging (DSI) scans were acquired using an echo planar imaging sequence, incorporating multiple b-values (TR = 3700 milliseconds, TE = 72 milliseconds, FOV = 220 mm × 220 mm, matrix = 110 × 110, slice thickness = 2 mm, number of slices = 66, and in-plane resolution = 2 mm). One hundred DWI volumes were obtained using a multiband sequence (Simultaneous Multi-Slice = 2, GRAPPA = 2). These volumes encompassed 12 b-values from b = 0 to b = 3000 seconds/mm^2 and 99 diverse diffusion encoding orientations.

Data processing

Diffusion data with b-values ranging from 0 to 1000 seconds/mm^2 were separated from the acquired DSI data using a custom MATLAB code (MATLAB 2016b, The Math Works, Inc.). Within this study's complete set of DSI data, those with b-values of 0-1000 seconds/mm^2 provided sufficient diffusion directions to reconstruct the DTI model. The FSL software (version 6.0.6.3, https://fsl.fmrib.ox.ac.uk/fsl/fslwiki) was used for eddy current correction, motion correction, and brain mask extraction. Additionally, component denoising and Gibbs-unringing[32] were performed using MRtrix3 (http://www.mrtrix3.org). The fractional anisotropy (FA) maps produced using FSL were subsequently converted into FA color maps using AFNI (https://afni.nimh.nih.gov/) to facilitate the direct delineation of ALPS regions of interest (ROIs) using tools such as ITK SNAP (http://www.itksnap.org). The above process was implemented using a custom Linux shell script, which functioned as a batch processor for the data of all subjects.

Regions of interest

Figure 1 shows the comparison of the dispersion of lateral ventricle horizontal projection fibers and association fibers along the PVS. The PVS's direction was perpendicular to the ventricle wall at the lateral ventricle level, resulting in its predominant alignment along the left and right directions (x-axis) in the axial plane. This direction is also perpendicular to the projection fibers (mainly on the z-axis) and the associated fibers (mainly on the y-axis; Figure 1A). Thus, in regions with projected/associated fibers, the diffuse nature along the x-axis represents at least partially the diffusion pattern along the perivascular space. A spherical ROI of 32 mm^3 was placed in the projection fibers (blue in Figure 1B) and association fibers (green in Figure 1B)[11]. The diffusivity for each ROI was calculated for both groups along the x, y, and z axes. In the case of projection fibers, the diffusivity was observed along the ROI x-axis, denoted as Dx-projection. In contrast, it was referred to as Dx-association in the association fiber regions. The diffusion coefficients of the projection fiber y-axis (Dy-projection) and association fiber z-axis (Dz-association) were also obtained.

Calculation of the DTI-ALPS index

The DTI-ALPS index, as proposed by Taoka *et al*[11], was determined by calculating the ratio of the average values of projection fibers (Dx-projection) and association fibers (Dx-association) along the x-axis to the average value of projection fibers (Dy-projection) along the y-axis and association fibers (Dz-association) along the z-axis. Mathematically, the DTI-ALPS index can be expressed as the DTI-ALPS index = mean (Dx-projection, Dx-association)/mean (Dy-projection, Dz-association).

Statistical analysis

Analysis of demographic data, inter-group comparisons, and correlation analysis were conducted using the R statistic software (version 4.2.3) (https://cran.r-project.org/). Pairwise comparisons for normally distributed variables were performed using the LSD method, while the Wilcoxon rank-sum test was employed for pairwise comparisons of non-normally distributed variables. Differences between the prediabetes group, the T2DM group, and the NGM group were assessed using one-way analysis of variance. The paired *t*-test was used to analyze the lateralization effect on DTI-ALPS indices within each group. Pearson's or Spearman's partial correlation analysis was used to assess the correlation between the DTI-ALPS index and clinical features. *P* values < 0.05 were considered indicative of statistical significance.

RESULTS

Demographics and clinical information

The demographic and clinical characteristics of participants in the three groups are summarized in Table 1. There were significant differences between the three groups with respect to FPG, 2hPG, HOMA-IR, and HbA1c levels ($P < 0.01$ after Bonferroni correction). However, there were no significant differences with respect to the other clinical features.

Comparison of DTI-ALPS indices between and within the three groups

There was no significant difference in the left-side ($P = 0.680$; Figure 2A), right-side ($P = 0.614$; Figure 2B), and mean ($P = 0.585$; Figure 2C) DTI-ALPS index between the prediabetes group and the NGM group. Compared with the NGM group, the left-side ($P = 0.025$, 95%CI: 1.646 to 1.918 *vs* 1.691 to 1.951; Figure 2A), right-side ($P = 0.002$, 95%CI: 1.655 to 1.943 *vs* 1.712 to 1.987; Figure 2B), mean ($P = 0.001$, 95%CI: 1.672 to 1.909 *vs* 1.722 to 1.949; Figure 2C) DTI-ALPS index were significantly reduced in the T2DM group. Compared with the prediabetes group, there was no significant difference in

Table 1 Demographic and clinical characteristics of the study population

Characteristics	NGM (*n* = 22)	Prediabetes (*n* = 20)	T2DM (*n* = 22)	*P* value	Bonferroni-adjusted *P* value
Age (years)	51.27 ± 6.80	49.70 ± 7.62	49.36 ± 7.42	0.65[3]	1
Female, *n* (%)	11 (50)	9 (45)	10 (45)	0.94[2]	1
Education (years)	14.50 ± 3.21	15.25 ± 3.00	14.41 ± 2.54	0.44[3]	1
BMI (kg/m^2)	23.38 ± 2.11	25.33 ± 3.35	25.75 ± 3.83	0.04[1]	1
Weight (kg)	62.39 ± 8.05	68.43 ± 13.59	69.30 ± 12.66	0.11[1]	1
Height (cm)	163.11 ± 5.29	163.78 ± 10.88	163.73 ± 7.14	0.96[1]	1
Waist (cm)	82.91 ± 5.13	87.88 ± 10.21	92.07 ± 10.09	0.004[1]	0.166
Hip (cm)	95.42 ± 3.90	96.43 ± 7.16	96.38 ± 7.19	0.84[1]	1
Waist-to-hip ration	0.87 ± 0.07	0.91 ± 0.07	0.95 ± 0.09	0.004[3]	0.151
Systolic BP (mmHg)	119.86 ± 15.63	124.10 ± 10.75	135.14 ± 23.94	0.026[3]	1
Diastolic BP (mmHg)	71.77 ± 13.80	76.25 ± 10.37	87.32 ± 21.32	0.009[3]	0.3792
TC (mmol/L)	5.27 ± 1.03	5.37 ± 0.93	5.73 ± 1.53	0.55[3]	1
TG (mmol/L)	1.82 ± 1.11	2.00 ± 1.60	3.15 ± 2.98	0.03[3]	1
HDL (mmol/L)	1.48 ± 0.40	1.34 ± 0.37	1.30 ± 0.32	0.32[3]	1
LDL (mmol/L)	2.88 ± 0.94	3.10 ± 0.89	3.18 ± 0.82	0.54[3]	1
FPG (mmol/L)	4.88 ± 0.28	5.54 ± 0.84	9.43 ± 7.39	< 0.001[3]	< 0.001
2hPG (mmol/L)	6.05 ± 1.21	9.20 ± 0.94	16.28 ± 6.72	< 0.001[3]	< 0.001
Fasting insulin (pmol/L)	56.09 ± 22.19	89.27 ± 59.74	101.32 ± 1.31	0.04[3]	1
HbA1c [mmol/mol (%)]	5.64 ± 0.42	6.01 ± 0.51	8.51 ± 3.42	< 0.001[3]	< 0.001
HOMA-IR	2.04 ± 0.87	3.87 ± 3.42	6.16 ± 5.29	0.002[3]	0.002
MMSE	29.77 ± 0.53	29.80 ± 0.41	29.00 ± 1.38	0.02[3]	0.79

[1]ANOVA test.
[2]Pearson's χ^2 test.
[3]Kruskal-Wallis rank sum test.
Continuous variables are expressed as mean ± SD and categorical variables are expressed as frequencies. NGM: Normal glucose metabolism; T2DM: Type 2 diabetes mellitus; BMI: Body mass index; BP: Blood pressure; TC: Total cholesterol; TG: Triglycerides; HDL: High-density lipoprotein; LDL: Low-density lipoprotein; FPG: Fasting plasma glucose; 2hPG: 2-hour postprandial glucose; HbA1c: Glycosylated hemoglobin; HOMA-IR: Homeostatic insulin resistance model; MMSE: Mini-mental state examination.

the left-side DTI-ALPS index of the T2DM group (P = 0.072; Figure 2A), but the right-side (P = 0.011, 95%CI: 1.401 to 1.676 *vs* 1.655 to 1.943; Figure 2B), and mean (P = 0.010, 95%CI: 1.461 to 1.687 *vs* 1.672 to 1.909; Figure 2C) DTI-ALPS index were significantly reduced.

There was no significant difference in DTI-ALPS index between the left-side and right-side basal ganglia in the NGM group (P = 0.704), prediabetes group (P = 0.849), and T2DM group (P = 0.224).

Differences in neuropsychological scores between the three groups

To examine the existence of cognitive impairment in the prediabetes and T2DM groups, we compared the neuropsychological scores between the three groups (Figure 3). There was no significant difference in the MMSE score between the prediabetes group and the NGM group (P = 0.956). However, the MMSE score of the T2DM group was significantly lower than that of the NGM group (P = 0.020, Z = -2.334) and prediabetes group (P = 0.025, Z = -2.254). After P-value correction, there was no significant decrease in MMSE score in the T2DM group compared with the NGM (P = 0.061) and prediabetes (P = 0.061) groups.

Correlation of DTI-ALPS index with clinical features

To investigate whether changes in the DTI-ALPS index were associated with clinical features, we assessed the correlation between the DTI-ALPS index and clinical features in the prediabetic group and T2DM group (Table 2).

After adjusting for sex, there was no significant correlation between the left-side (r = -0.197, P = 0.418), right-side (r = -0.336, P = 0.160), and mean DTI-ALPS (r = -0.350, P = 0.142) index and the MMSE score in the prediabetes group, and there was no significant correlation between the left-side (r = -0.117, P = 0.614), right-side (r = 0.106, P = 0.646), and mean

Table 2 Correlations between clinical features and biomarkers of the glymphatic system in prediabetes and type 2 diabetes mellitus

Characteristic	Prediabetes (*n* = 20)			T2DM (*n* = 22)		
	L-DTI-ALPS (95%CI)	R-DTI-ALPS (95%CI)	Mean-DTI-ALPS (95%CI)	L-DTI-ALPS (95%CI)	R-DTI-ALPS (95%CI)	Mean-DTI-ALPS (95%CI)
Age	-0.215 (-0.540, 0.234)[1]	-0.353 (-0.660, 0.076)[1]	-0.357 (-0.642, -0.020)[1]	-0.136 (-0.525, 0.244)[1]	-0.068 (-0.460, 0.344)[1]	-0.105 (-0.510, 0.277)[1]
Education years	0.242 (-0.385, 0.732)[2]	0.108 (-0.552, 0.600)[2]	0.227 (-0.457, 0.737)[2]	0.214 (-0.327, 0.676)[2]	0.027 (-0.510, 0.496)[2]	0.048 (-0.483, 0.544)[2]
BMI	-0.075 (-0.514, 0.404)[1]	-0.146 (-0.593, 0.394)[1]	-0.140 (-0.590, 0.326)[1]	0.161 (-0.245, 0.501)[1]	0.115 (-0.250, 0.516)[1]	0.147 (-0.270, 0.549)[1]
Weight	0.169 (-0.386, 0.477)[1]	-0.104 (-0.499, 0.466)[1]	0.034 (-0.450, 0.406)[1]	0.327 (0.005, 0.558)[1]	0.323 (0.068, 0.586)[1]	0.357 (0.095, 0.579)[1]
Height	0.332 (-0.364, 0.653)[1]	0.100 (-0.547, 0.540)[1]	0.264 (-0.434, 0.636)[1]	0.554 (-0.142, 0.822)[1,b]	0.621 (0.096, 0.828)[1,b]	0.651 (0.016, 0.853)[1,b]
Waist	-0.153 (-0.583, 0.314)[1]	-0.198 (-0.567, 0.441)[1]	-0.220 (-0.582, 0.298)[1]	0.376 (-0.022, 0.667)[1]	0.130 (-0.190, 0.481)[1]	0.255 (-0.129, 0.576)[1]
Hip	-0.077 (-0.469, 0.393)[1]	0.184 (-0.264, 0.581)[1]	0.073 (-0.346, 0.478)[1]	0.370 (0.011, 0.661)[1]	0.230 (-0.139, 0.639)[1]	0.316 (-0.002, 0.651)[1]
Waist-to-hip ratio	-0.152 (-0.658, 0.349)[2]	-0.495 (-0.784, 0.017)[2,a]	-0.467 (-0.770, 0.067)[2,a]	0.326 (-0.147, 0.671)[2]	0.124 (-0.388, 0.547)[2]	0.298 (-0.275, 0.673)[2]
Systolic BP (mmHg)	-0.204 (-0.634, 0.276)[2]	-0.168 (-0.551, 0.277)[2]	-0.203 (-0.701, 0.261)[2]	0.086 (-0.410, 0.536)[2]	0.152 (-0.380, 0.587)[2]	0.105 (-0.437, 0.560)[2]
Diastolic BP (mmHg)	-0.029 (-0.436, 0.515)[2]	-0.242 (-0.634, 0.188)[2]	-0.147 (-0.563, 0.323)[2]	0.193 (-0.338, 0.581)[2]	-0.162 (-0.653, 0.326)[2]	0.004 (-0.521, 0.460)[2]
TC	-0.567 (-0.831, -0.152)[2,a]	-0.107 (-0.584, 0.389)[2]	-0.411 (-0.734, 0.042)[2]	0.043 (-0.442, 0.510)[2]	-0.098 (-0.577, 0.434)[2]	-0.056 (-0.559, 0.454)[2]
TG	0.035 (-0.527, 0.555)[2]	-0.160 (-0.654, 0.323)[2]	-0.140 (-0.675, 0.390)[2]	0.151 (-0.296, 0.581)[2]	0.093 (-0.447, 0.538)[2]	0.128 (-0.353, 0.614)[2]
HDL	-0.294 (-0.720, 0.235)[2]	0.214 (-0.302, 0.637)[2]	-0.039 (-0.564, 0.416)[2]	-0.544 (-0.792, -0.109)[2,a]	-0.409 (-0.717, 0.070)[2]	-0.544 (-0.802, -0.013)[2,a]
LDL	-0.545 (-0.801, -0.022)[2,a]	-0.186 (-0.674, 0.338)[2]	-0.443 (-0.792, 0.022)[2]	0.148 (-0.408, 0.573)[2]	-0.047 (-0.530, 0.484)[2]	0.046 (-0.474, 0.506)[2]
FPG	-0.270 (-0.681, 0.372)[2]	-0.343 (-0.712, 0.113)[2]	-0.410 (-0.750, 0.134)[2]	0.138 (-0.228, 0.573)[2]	0.235 (-0.234, 0.567)[2]	0.226 (-0.217, 0.555)[2]
2hPG	0.582 (0.192, 0.830)[2,a]	0.193 (-0.428, 0.673)[2]	0.477 (-0.103, 0.797)[2,a]	-0.182 (-0.657, 0.332)[2]	-0.348 (-0.689, 0.254)[2]	-0.380 (-0.731, 0.151)[2]
HbA1c	-0.325 (-0.690, 0.227)[2]	-0.662 (-0.867, -0.122)[2,b]	-0.725 (-0.886, -0.398)[2,b]	-0.036 (-0.439, 0.376)[2]	0.251 (-0.329, 0.653)[2]	0.175 (-0.326, 0.513)[2]
Fasting insulin	0.152 (-0.298, 0.550)[2]	-0.265 (-0.646, 0.156)[2]	-0.057 (-0.503, 0.363)[2]	0.091 (-0.384, 0.463)[2]	-0.069 (-0.519, 0.420)[2]	-0.006 (-0.473, 0.415)[2]
HOMA-IR	0.115 (-0.339, 0.582)[2]	-0.286 (-0.640, 0.201)[2]	-0.100 (-0.525, 0.367)[2]	0.140 (-0.347, 0.576)[2]	0.035 (-0.455, 0.474)[2]	0.094 (-0.419, 0.505)[2]
MMSE	-0.197 (-0.678, 0.450)[2]	-0.336 (-0.725, 0.355)[2]	-0.350 (-0.740, 0.540)[2]	-0.117 (-0.596, 0.316)[2]	0.106 (-0.411, 0.595)[2]	0.065 (-0.420, 0.515)[2]

[a]$P < 0.05$.

[b]$P < 0.01$.

[1]Pearson correlation coefficient.

[2]Spearman correlation coefficient.

Results are expressed as correlation coefficients and 95%CI. DTI-ALPS: Diffusion tensor image analysis method along the perivascular space; L-DTI-ALPS: Diffusion tensor image analysis method along the perivascular space index of the left cerebral hemisphere in prediabetes and type 2 diabetes; R-DTI- ALPS: Diffusion tensor image analysis method along the perivascular space index of the right cerebral hemisphere of prediabetes and type 2 diabetes; Mean-DTI-ALPS: Mean diffusion tensor image analysis method along the perivascular space index in both cerebral hemispheres; T2DM: Type 2 diabetes mellitus; NGM: Normal glucose metabolism; BMI: Body mass index; BP: Blood pressure; TC: Total cholesterol; TG: Triglycerides; HDL: High-density lipoprotein; LDL: Low-density lipoprotein; FPG: Fasting plasma glucose; 2hPG: 2-hour postprandial glucose; HbA1c: Glycosylated hemoglobin; HOMA-IR: Homeostatic insulin resistance model; MMSE: Mini-mental state examination.

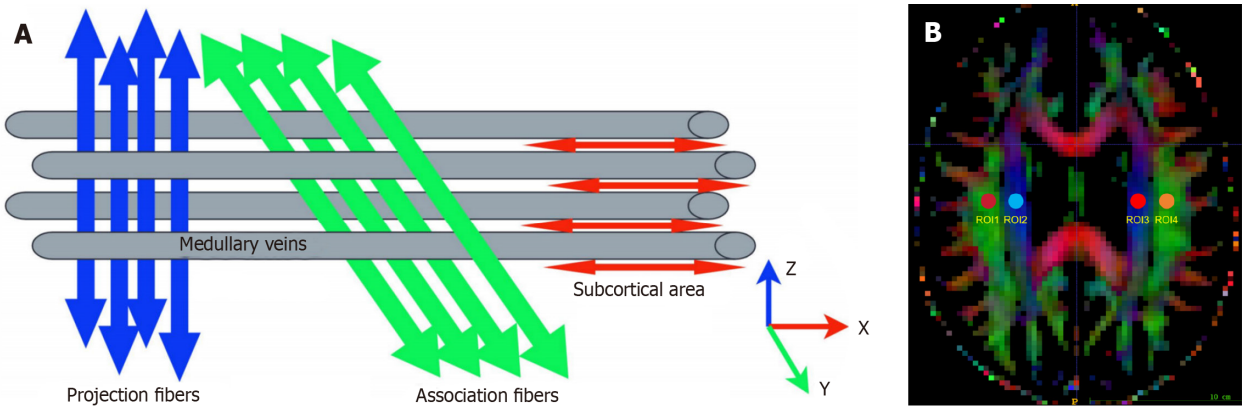

Figure 1 Schematic illustration of the diffusion tensor image analysis method along the perivascular space. A: Schematic diagram showing the relationship between the direction of the perivascular space (gray cylinder) and the direction of the projection fibers (blue) and association fibers (green). Note that the orientation of the perivascular space is perpendicular to the projection and association fibers; B: Diffusion tensor image superimposed color shows the distribution of projection fibers (z-axis: Blue) and association fibers (y-axis: Green). Four regions of interest were placed on both sides of the projection fibers (projection region) and the association fibers (association region) to measure the diffusion coefficients in the three directions (x, y, and z axes).

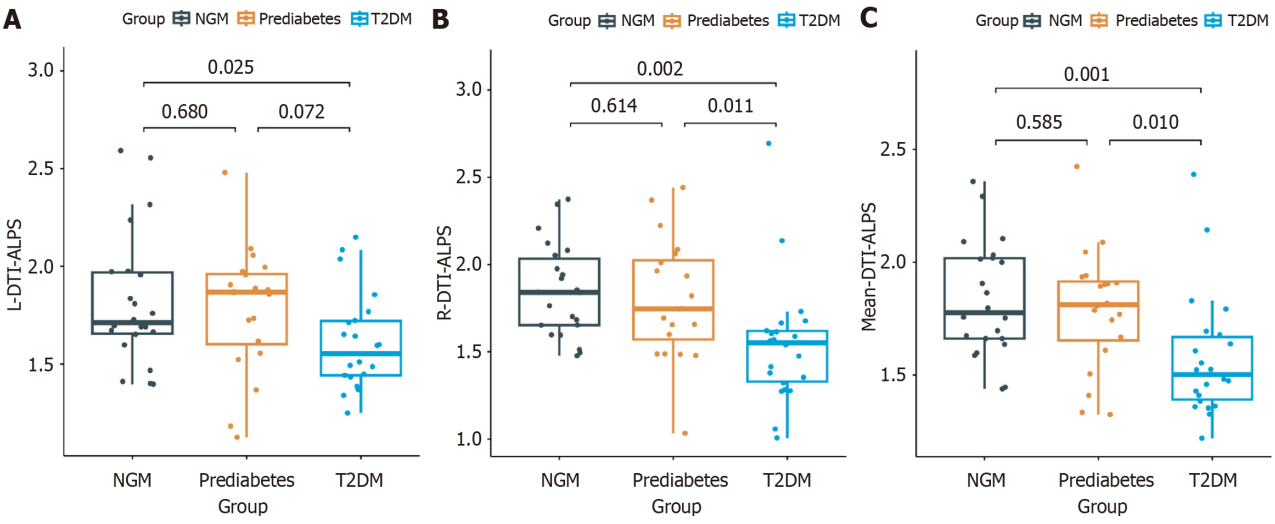

Figure 2 The left-side\right-side\mean diffusion tensor image analysis method along the perivascular space index was evaluated. A: The diffusion tensor image analysis method along the perivascular space (DTI-ALPS) index of the left-side cerebral hemisphere in patients with type 2 diabetes mellitus (T2DM) was significantly lower than in the normal glucose metabolism (NGM) group; B: The DTI-ALPS index of the right cerebral hemisphere in patients with T2DM was significantly lower than that in the prediabetes group and the NGM group; C: The mean DTI-ALPS index of both cerebral hemispheres in patients with T2DM was significantly higher in the prediabetes and NGM groups. T2DM: Type 2 diabetes mellitus; NGM: Normal glucose metabolism; DTI-ALPS: Diffusion tensor image analysis method along the perivascular space; L-DTI-ALPS: Diffusion tensor image analysis method along the perivascular space index of the left cerebral hemisphere in prediabetes and type 2 diabetes mellitus; R-DTI-ALPS: Diffusion tensor image analysis method along the perivascular space index of the right cerebral hemisphere of prediabetes and type 2 diabetes mellitus; Mean-DTI-ALPS: Mean Diffusion tensor image analysis method along the perivascular space index in both cerebral hemispheres.

DTI-ALPS (r = 0.065, P = 0.781) index and the MMSE score in the T2DM group. However, in the prediabetes group, after adjusting for sex, there was a positive correlation between the left-side DTI-ALPS index and 2hPG (r = 0.582, P = 0.009, 95%CI: 0.192 to 0.830; Figure 4A). In contrast, negative correlations were observed with TC (r = -0.567, P = 0.011, 95%CI: -0.831 to -0.152; Figure 4B) and LDL (r = -0.545, P = 0.016, 95%CI: -0.720 to 0.235; Figure 4C). In the prediabetes group, the right-side DTI-ALPS index exhibited a negative correlation with waist-to-hip ratio (r = -0.495, P = 0.031, 95%CI: -0.784 to 0.017; Figure 4D) and HbA1c level (r = -0.662, P = 0.002, 95%CI: -0.867 to -0.122; Figure 4E). Additionally, the mean DTI-ALPS index in the prediabetes group showed a negative correlations with waist-to-hip ratio (r = -0.467, P = 0.044, 95%CI: -0.770 to 0.067; Figure 4F) and HbA1c level (r = -0.725, P = 0.0004, 95%CI: -0.886 to -0.398; Figure 4G), as well as positive correlation with 2hPG (r = 0.477, P = 0.039, 95%CI: -0.103 to 0.797; Figure 4H). In the T2DM group, the left-side DTI-ALPS index exhibited a positive correlation with height (r = 0.553, P = 0.009, 95%CI: -0.142 to 0.822; Figure 4I), while it demonstrated a negative correlation with HDL level (r = -0.548, P = 0.010, 95%CI: -0.792 to -0.109; Figure 4J). Similarly, the right DTI-ALPS index in the T2DM group displayed a positive correlation with height (r = 0.621, P = 0.003, 95%CI: 0.096 to 0.828; Figure 4K). Furthermore, the mean DTI-ALPS index of the T2DM group was positively correlated with height (r = 0.651, P = 0.001, 95%CI: 0.016 to 0.853; Figure 4L) and negatively correlated with HDL (r = -0.544, P = 0.010, 95%CI: -

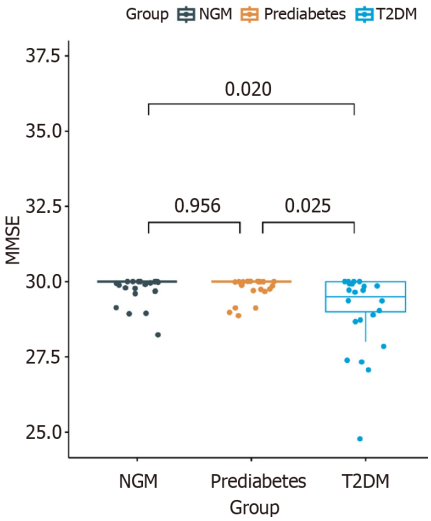

Figure 3 The mini-mental state examination score in the type 2 diabetes mellitus group was significantly lower than that in the normal glucose metabolism and prediabetic groups. T2DM: Type 2 diabetes mellitus; NGM: Normal glucose metabolism; MMSE: The mini-mental state examination.

0.802 to -0.013; Figure 4M).

DISCUSSION

The DTI-ALPS index, a novel noninvasive marker for evaluating glymphatic function, was employed in this study utilizing the 3.0 Tesla MRI. There were no significant differences in the left-side, right-side, and mean DTI-ALPS indices between the prediabetic group and the NGM group. However, the T2DM group exhibited significantly lower left-side, right-side, and mean DTI-ALPS index compared to the NGM group. Furthermore, the right-side and mean DTI-ALPS index in the T2DM group were significantly lower than that on the corresponding side of the prediabetic group. These findings indicate variations in glymphatic function across different glucose metabolism states. This study found no left-right differentiation within the group. The MMSE score of individuals with T2DM was notably lower compared to those with NGM and prediabetes. However, the MMSE score showed no significant correlation with the DTI-ALPS index after adjusting for sex. Furthermore, distinct clinical indicators were found to influence the DTI-ALPS index in individuals with prediabetes and T2DM. These findings indicate that DTI-ALPS index is a potential tool for evaluating glymphatic function in individuals with prediabetes and T2DM.

This study employed a 3.0 T MRI to examine the DTI-ALPS in individuals diagnosed with prediabetes and T2DM. The DTI-ALPS index was determined by assessing the diffusion ratio along the medullary vein's PVS to diffusion perpendicular to the primary fiber tract direction[11,33]. While the DTI-ALPS primarily focuses on measuring and evaluating diffusion abnormalities near the PVS, it can partially represent the overall glymphatic function[11,33].

Prediabetes and T2DM glymphatic function

Chronic hyperglycemia can potentially modify the water diffusion characteristics in brain tissue. Furthermore, chronic hyperglycemia over an extended period can impact synapse formation, intensify the body's response to oxidative stress, and lead to the accumulation of advanced glycation end products. Additionally, it can expedite the development of atherosclerotic plaques, which in turn can cause neuronal and vascular injury. These effects increase the incidence of peripheral vascular complications[17,34].

Furthermore, the deposition and elimination of Aβ and tau proteins can potentially impact the properties of tissue water diffusion[35]. This phenomenon may potentially account for the alteration in the DTI-ALPS index induced by chronic hyperglycemia. Notably, we found no significant decrease in the DTI-ALPS index among individuals with prediabetes compared to those with NGM. However, the DTI-ALPS index in the T2DM group was significantly decreased compared to the NGM group. Additionally, the right-side and mean DTI-ALPS index in the T2DM group were significantly decreased compared to the prediabetic group, which is consistent with the findings of Yang *et al*[19]. The decline in the DTI-ALPS index may be ascribed to the association between T2DM and atherosclerosis[36-38], which promotes the aggregation of Aβ and tau proteins. Hence, glymphatic dysfunction primarily manifests in individuals with T2DM across various glucose metabolism states. Nevertheless, the precise mechanisms responsible for glymphatic impairment in different glucose metabolic states are not clear. Potential factors contributing to this impairment include reduced arterial pulses, heightened PVS, modified expression and distribution of AQP4, or astrocyte swelling[19,39]. Additional research is required to ascertain the impact of various physiological lymphokines, including meningeal glymphatic and venous outflow and CSF production rates, on glymphatic function following an ischemic stroke (IS)[40]. Moreover, further investigations are required to identify potential glymphatic impairments in different stages of impaired

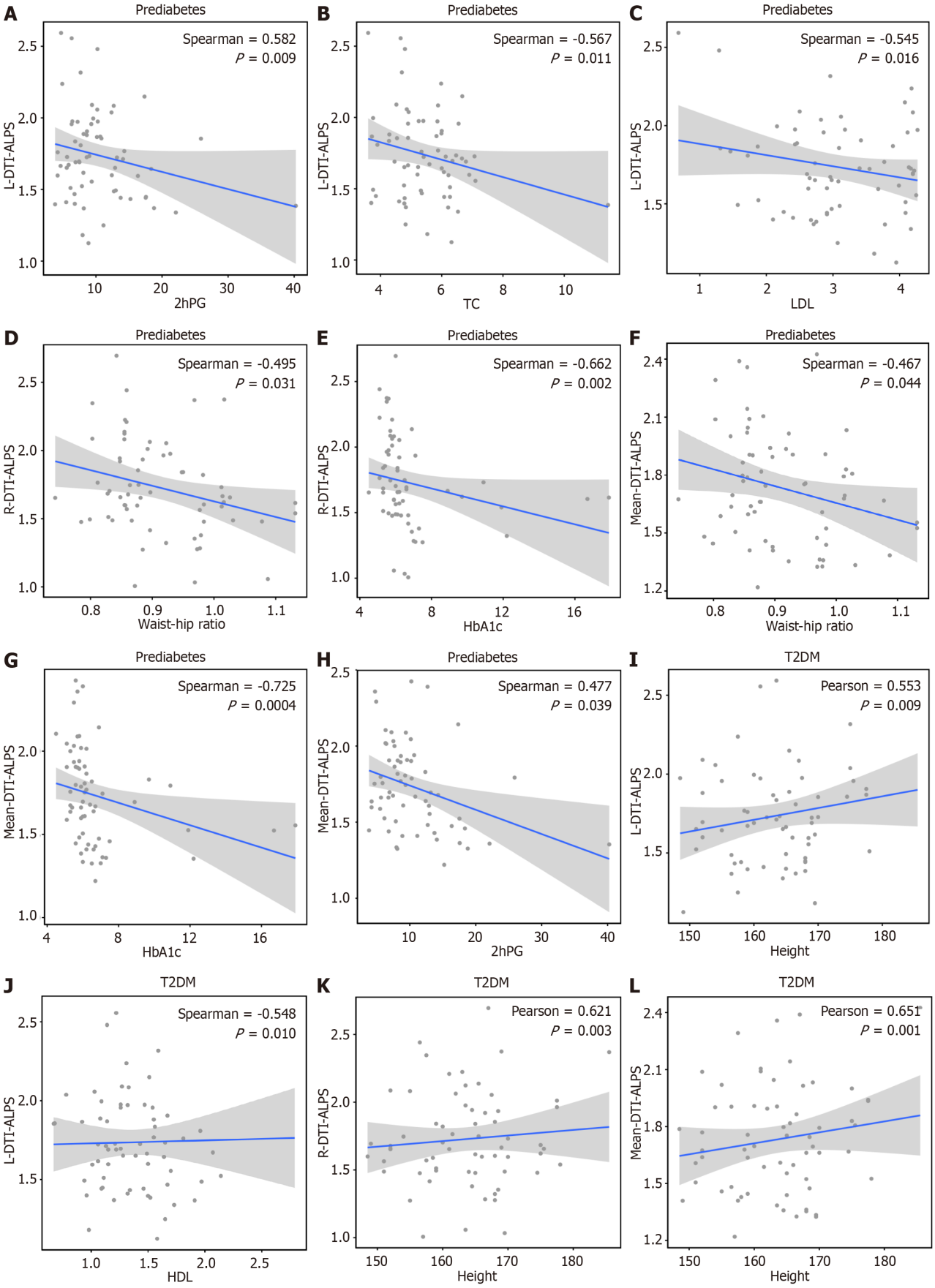
A
Prediabetes
Spearman = 0.582
P = 0.009
L-DTI-ALPS
2hPG
B
Prediabetes
Spearman = -0.567
P = 0.011
L-DTI-ALPS
TC
C
Prediabetes
Spearman = -0.545
P = 0.016
L-DTI-ALPS
LDL
D
Prediabetes
Spearman = -0.495
P = 0.031
R-DTI-ALPS
Waist-hip ratio
E
Prediabetes
Spearman = -0.662
P = 0.002
R-DTI-ALPS
HbA1c
F
Prediabetes
Spearman = -0.467
P = 0.044
Mean-DTI-ALPS
Waist-hip ratio
G
Prediabetes
Spearman = -0.725
P = 0.0004
Mean-DTI-ALPS
HbA1c
H
Prediabetes
Spearman = 0.477
P = 0.039
Mean-DTI-ALPS
2hPG
I
T2DM
Pearson = 0.553
P = 0.009
L-DTI-ALPS
Height
J
T2DM
Spearman = -0.548
P = 0.010
L-DTI-ALPS
HDL
K
T2DM
Pearson = 0.621
P = 0.003
R-DTI-ALPS
Height
L
T2DM
Pearson = 0.651
P = 0.001
Mean-DTI-ALPS
Height

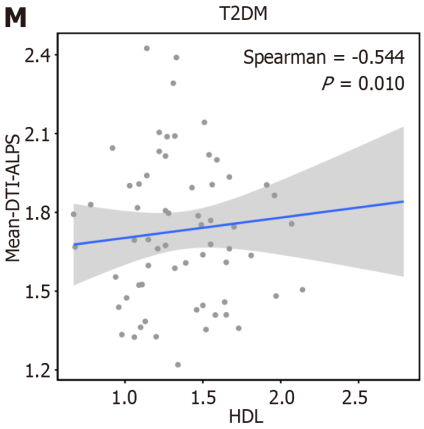

Figure 4 The correlation between the diffusion tensor image analysis method along the perivascular space index and other clinical features. A: The left-side diffusion tensor image analysis method along the perivascular space (DTI-ALPS) index in the prediabetes group was positively correlated with 2-hour postprandial glucose (2hPG) (r = 0. 582, P = 0.009, 95%CI: 0.192 to 0.830); B and C:The left-side DTI-ALPS index in the prediabetes group was negatively correlated with total cholesterol (r = -0.567, P = 0.011, 95%CI: -0.831 to -0.152) and low-density lipoprotein (r = -0.545, P = 0.016, 95%CI: -0.720 to 0.235); D and E: The right-side DTI-ALPS index in the prediabetes group was negatively correlated with waist-to-hip ratio (r = -0. 495, P = 0.031, 95%CI: -0.784 to 0.017) and glycosylated hemoglobin (HbA1c) (r = -0.662, P = 0.002, 95%CI: -0.867 to -0.122); F and G: The mean DTI-ALPS index in the prediabetes group negatively correlated with waist-to-hip ratio (r = -0.467, P = 0.044, 95%CI: -0.770 to 0.067) and HbA1c (r = -0.725, P = 0.0004, 95%CI: -0.886 to -0.398); H:The mean DTI-ALPS index in the prediabetes group was positively correlated with 2hPG (r = 0.477, P = 0.039, 95%CI: -0.103 to 0.797); I: The left-side DTI-ALPS index in the type 2 diabetes mellitus (T2DM) group was positively correlated with height (r = 0.553, P = 0.009, 95%CI: -0.142 to 0.822); J: The left-side DTI-ALPS index in the T2DM group was negatively correlated with high-density lipoprotein (HDL) (r = -0.548, P = 0.010, 95%CI: -0.792 to -0.109); K: The right-side DTI-ALPS index in the T2DM group was positively correlated with height (r = 0.621, P = 0.003, 95%CI: 0.096 to 0.828); L: The mean DTI-ALPS index of the T2DM group was positively correlated with height (r = 0.651, P = 0.001, 95%CI: 0.016 to 0.853); M: The mean DTI-ALPS index in the T2DM group negatively correlated with HDL (r = -0.544, P = 0.010, 95%CI: -0.802 to -0.013). T2DM: Type 2 diabetes mellitus; NGM: Normal glucose metabolism; DTI-ALPS: Diffusion tensor image analysis method along the perivascular space; L-DTI-ALPS: Diffusion tensor image analysis method along the perivascular space index of the left cerebral hemisphere in prediabetes and type 2 diabetes mellitus; R-DTI-ALPS: Diffusion tensor image analysis method along the perivascular space index of the right cerebral hemisphere of prediabetes and type 2 diabetes mellitus; Mean-DTI-ALPS: Mean Diffusion tensor image analysis method along the perivascular space index in both cerebral hemispheres; 2hPG: 2-hour postprandial glucose; TC: Total cholesterol; LDL: Low-density lipoprotein; HbA1c: Glycosylated hemoglobin; HDL: High-density lipoprotein.

glucose metabolism and establish therapeutic interventions for addressing such impairments.

In contrast to prior investigations, the present study did not observe exponential lateralization of DTI-ALPS among the three groups[17,19,41]. Due to the limited sample sizes in various studies and the heterogeneity of the diseases under examination, ascertaining the lateralizing effects in the glymphatic system of the human brain is challenging. Furthermore, the thickness of the superior longitudinal fasciculus is influenced by chirality and dominant cerebral flanks [42]. These factors can potentially impact the measurement of the DTI-ALPS index, thereby compromising the accuracy of the obtained results. Due caution should be exercised when addressing present manifestations of laterality. Further studies are required to clarify the presence and underlying factors of laterality within the glymphatic system.

Impaired cognitive function in different glucose metabolic states

This study observed a notable decline in MMSE scores in the T2DM group compared to the NGM and prediabetes groups. Although the difference was insignificant after *post hoc* correction of the P values, it showed a trend. While diabetes is widely recognized as a risk factor for dementia, the potential effect of prediabetes in causing cognitive decline has been debated[7,43,44]. This study did not identify any significant difference between the prediabetic and NGM groups in this respect. However, given the limited sample size and the cross-sectional study design, a multicenter study with a larger sample size is required to validate the findings regarding the potential decline in cognitive function among individuals with prediabetes. It is worth mentioning that our findings align with previous research in the T2DM phase [45-47]. Glucose dysregulation is implicated in the onset and advancement of neurological and cognitive complications associated with diabetes[48]. Nevertheless, various longitudinal studies investigating the impact of diabetes-related cognitive decline have yielded inconclusive results[44,49,50]. These studies were limited by their relatively short follow-up periods and incomplete prediabetes or glycemic control evaluation, potentially accounting for the discrepancies observed in the outcomes above.

Relationship between DTI-ALPS index and clinical features in patients with different glucose metabolism

Previous studies have demonstrated a positive correlation between the DTI-ALPS index and MMSE scores[17,18,51]. In the present study, although MMSE scores were significantly lower in the T2DM group than in the NGM and prediabetes groups, no correlation was found between the left-side, right-side, and mean DTI-ALPS indices of the prediabetes and T2DM groups and MMSE scores. This may be attributed to this small sample size and cross-sectional study design. Multicenter studies with a larger sample size are required to validate the correlation between the DTI-ALPS index and MMSE among diabetic patients.

The DTI-ALPS index is an approximate gauge for evaluating glymphatic function, although factors other than glymphatic dysfunction can influence its variations. In this study, the main variables impacting the DTI-ALPS index in individuals with prediabetes were 2hPG, TC, LDL, waist-to-hip ratio, and HbA1c level. Conversely, the key factors influencing the DTI-ALPS index in patients with T2DM were height and HDL level. Of note, a positive correlation was observed between the left-side DTI-ALPS index and 2hPG in the prediabetes group. This association could be attributed to the fact that the glucose concentration in CSF depends on the glucose levels in the peripheral blood[52]. The CSF is present within the perivascular brain tissue, specifically within the PVS. In individuals with prediabetes, the glymphatic system, which is responsible for clearing waste from the brain, remains functional to manage increased blood glucose levels within the perivascular inter fluid in the basal ganglia. While the DTI-ALPS index in the prediabetes group showed a positive correlation with 2hPG levels, it exhibited a negative correlation with HbA1c levels. HbA1c is an indirect measure of the average blood glucose concentration over the past three months and does not reflect short-term glycemic control[53]. Hence, despite the inverse association between the prediabetic DTI-ALPS index and 2hPG, a positive correlation was found with HbA1c. Numerous studies have indicated that elevated levels of LDL and TC increase the susceptibility to cardiovascular disease[54,55] and the development of atherosclerosis. In the prediabetes group, a negative correlation of DTI-ALPS index with LDL and TC was observed, potentially indicating a link to LDL and TC-induced arteriosclerosis. The waist-to-hip ratio is a highly sensitive indicator of fat accumulation and cardiovascular disease, surpassing the BMI's predictive capacity[56,57]. In this study, prediabetic individuals with a greater waist-to-hip ratio exhibited a diminished DTI-ALPS index, indirectly suggesting an increased likelihood of developing glymphatic dysfunction. Furthermore, within the T2DM group, a higher DTI-ALPS index was associated with lower levels of HDL, a biomarker known for its anti-inflammatory properties and consequential health benefits[58]. However, several studies have shown that comorbidities may potentially alter the composition and functionality of HDL particles, impeding their beneficial effects and potentially leading to harmful consequences[59-63]. The present study found a positive correlation between height and the DTI-ALPS index. Given the scarcity of comparable studies and the limited sample size in this study, the association between height and the DTI-ALPS index needs to be investigated in a larger multicenter study.

One notable aspect of this study was its utilization of the DTI-ALPS index to assess the functioning of the brain's glymphatic system among individuals with different glucose metabolism states while also investigating the clinical characteristics that impact the DTI-ALPS index. Our findings indicate that glymphatic dysfunction primarily manifests during T2DM. Based on the aforementioned preliminary findings, we posit that the DTI-ALPS index may serve as a useful marker for assessing the condition of the glymphatic system in individuals with different glucose metabolism states. Nevertheless, more robust studies with larger sample sizes are imperative to substantiate this preliminary assertion.

Some limitations of this study should be acknowledged. Due to the small sample size, the findings should be interpreted with caution. Secondly, due to multiple b-value acquisitions, the DSI acquisition method may be deemed the most optimal DTI-ALPS scanning protocol. This assertion is supported by a recent study[41,64], which demonstrated a strong correlation among DTI-ALPS values obtained through varying scan parameters, affirming the feasibility of conducting this study using our research protocol. Additionally, this study only collected 25 clinical features for correlation analysis. Further study is required to investigate the impact of drugs on the DTI-ALPS index. Moreover, future studies should include a broader range of clinical features to investigate their potential impact on DTI-ALPS.

CONCLUSION

In this study, among the different states of glucose metabolism, impairment of the glymphatic system was mainly observed during the stage of T2DM. Furthermore, the determinants of the DTI-ALPS index were found to differ between the prediabetes and T2DM stages. These findings suggest that the DTI-ALPS index is a potential tool for functional assessment of the brain's glymphatic system across different glucose metabolism states. Our findings enhance our understanding of the pathophysiology of diabetic brain damage and provide potential biological evidence for its early diagnosis.

FOOTNOTES

Author contributions: Tian B and Zeng ZS designed and interpreted the complete data and were major contributors to writing the manuscript; Liang JL, Gong JN, Xu YF, and Lu ST helped to acquire the magnetic resonance images; Zheng HL and Zhou J helped to acquire the clinical data; Zhao C and Zhang HT assisted in processing the magnetic resonance images; Tian B was responsible for data analysis and manuscript writing; Zeng ZS was responsible for funding support and supervised the study; All authors read and approved the final manuscript.

Institutional review board statement: The participants in this study (No. 2023-K118-01) consisted of human individuals and were subjected to review and approval by the Medical Ethics Committee of The First Affiliated Hospital of Guangxi Medical University. This study has been registered in the Chinese Clinical Trial Registry (https://www.chictr.org.cn/bin/project/edit?pid=199727) with registration number ChiCTR2300075515 (date of registration:07/09/2023).

Informed consent statement: Before their involvement, the subjects provided their informed consent by signing a consent form, expressing their agreement to participate in the study.

Conflict-of-interest statement: The authors declare that this study was conducted without any business or financial relationship that could be interpreted as a potential conflict of interest.

Data sharing statement: Subject to the Research Ethics Committee's discretion, clinical and neuroimaging data may be shared through contact communication channels upon reasonable request from a qualified investigator.

STROBE statement: The authors have read the STROBE Statement—checklist of items, and the manuscript was prepared and revised according to the STROBE Statement—checklist of items.

Country of origin: China

ORCID number: Bin Tian 0000-0003-2554-2650; Zi-San Zeng 0000-0002-6977-1175.

S-Editor: Li L
L-Editor: A
P-Editor: Che XX

REFERENCES

1 **Cho NH**, Shaw JE, Karuranga S, Huang Y, da Rocha Fernandes JD, Ohlrogge AW, Malanda B. IDF Diabetes Atlas: Global estimates of diabetes prevalence for 2017 and projections for 2045. *Diabetes Res Clin Pract* 2018; **138**: 271-281 [PMID: 29496507 DOI: 10.1016/j.diabres.2018.02.023]
2 **Zhou X**, Yu D, Sun X. Hypoxia-inducible factor-1α in diabetic foot ulcers: Plain but not simple. *Gene Expression* 2023; **22**: 306-320 [DOI: 10.14218/GE.2023.00051]
3 **Qin Y**, Zhang J, Babapoor-Farrokhran S, Applewhite B, Deshpande M, Megarity H, Flores-Bellver M, Aparicio-Domingo S, Ma T, Rui Y, Tzeng SY, Green JJ, Canto-Soler MV, Montaner S, Sodhi A. PAI-1 is a vascular cell-specific HIF-2-dependent angiogenic factor that promotes retinal neovascularization in diabetic patients. *Sci Adv* 2022; **8**: eabm1896 [PMID: 35235351 DOI: 10.1126/sciadv.abm1896]
4 **Gregg EW**, Sattar N, Ali MK. The changing face of diabetes complications. *Lancet Diabetes Endocrinol* 2016; **4**: 537-547 [PMID: 27156051 DOI: 10.1016/S2213-8587(16)30010-9]
5 **Prince M**, Wimo A, Guerchet M, Ali GC, Wu YT, Prina M. World Alzheimer Report 2015. The Global Impact of Dementia. London: Alzheimer's Disease International (ADI). Aug 2015. [cited 23 May 2024]. Available from: https://www.alzint.org/u/WorldAlzheimerReport2015.pdf
6 **Okereke OI**, Kang JH, Cook NR, Gaziano JM, Manson JE, Buring JE, Grodstein F. Type 2 diabetes mellitus and cognitive decline in two large cohorts of community-dwelling older adults. *J Am Geriatr Soc* 2008; **56**: 1028-1036 [PMID: 18384580 DOI: 10.1111/j.1532-5415.2008.01686.x]
7 **Marseglia A**, Fratiglioni L, Kalpouzos G, Wang R, Bäckman L, Xu W. Prediabetes and diabetes accelerate cognitive decline and predict microvascular lesions: A population-based cohort study. *Alzheimers Dement* 2019; **15**: 25-33 [PMID: 30114414 DOI: 10.1016/j.jalz.2018.06.3060]
8 **Iliff JJ**, Chen MJ, Plog BA, Zeppenfeld DM, Soltero M, Yang L, Singh I, Deane R, Nedergaard M. Impairment of glymphatic pathway function promotes tau pathology after traumatic brain injury. *J Neurosci* 2014; **34**: 16180-16193 [PMID: 25471560 DOI: 10.1523/JNEUROSCI.3020-14.2014]
9 **Klostranec JM**, Vucevic D, Bhatia KD, Kortman HGJ, Krings T, Murphy KP, terBrugge KG, Mikulis DJ. Current Concepts in Intracranial Interstitial Fluid Transport and the Glymphatic System: Part I-Anatomy and Physiology. *Radiology* 2021; **301**: 502-514 [PMID: 34665028 DOI: 10.1148/radiol.2021202043]
10 **Steward CE**, Venkatraman VK, Lui E, Malpas CB, Ellis KA, Cyarto EV, Vivash L, O'Brien TJ, Velakoulis D, Ames D, Masters CL, Lautenschlager NT, Bammer R, Desmond PM. Assessment of the DTI-ALPS Parameter Along the Perivascular Space in Older Adults at Risk of Dementia. *J Neuroimaging* 2021; **31**: 569-578 [PMID: 33556226 DOI: 10.1111/jon.12837]
11 **Taoka T**, Masutani Y, Kawai H, Nakane T, Matsuoka K, Yasuno F, Kishimoto T, Naganawa S. Evaluation of glymphatic system activity with the diffusion MR technique: diffusion tensor image analysis along the perivascular space (DTI-ALPS) in Alzheimer's disease cases. *Jpn J Radiol* 2017; **35**: 172-178 [PMID: 28197821 DOI: 10.1007/s11604-017-0617-z]
12 **Ulv Larsen SM**, Landolt HP, Berger W, Nedergaard M, Knudsen GM, Holst SC. Haplotype of the astrocytic water channel AQP4 is associated with slow wave energy regulation in human NREM sleep. *PLoS Biol* 2020; **18**: e3000623 [PMID: 32369477 DOI: 10.1371/journal.pbio.3000623]
13 **Ringstad G**, Vatnehol SAS, Eide PK. Glymphatic MRI in idiopathic normal pressure hydrocephalus. *Brain* 2017; **140**: 2691-2705 [PMID: 28969373 DOI: 10.1093/brain/awx191]
14 **Iliff JJ**, Wang M, Liao Y, Plogg BA, Peng W, Gundersen GA, Benveniste H, Vates GE, Deane R, Goldman SA, Nagelhus EA, Nedergaard M. A paravascular pathway facilitates CSF flow through the brain parenchyma and the clearance of interstitial solutes, including amyloid β. *Sci Transl Med* 2012; **4**: 147ra111 [PMID: 22896675 DOI: 10.1126/scitranslmed.3003748]
15 **Jessen NA**, Munk AS, Lundgaard I, Nedergaard M. The Glymphatic System: A Beginner's Guide. *Neurochem Res* 2015; **40**: 2583-2599 [PMID: 25947369 DOI: 10.1007/s11064-015-1581-6]
16 **Chen HL**, Chen PC, Lu CH, Tsai NW, Yu CC, Chou KH, Lai YR, Taoka T, Lin WC. Associations among Cognitive Functions, Plasma DNA,

and Diffusion Tensor Image along the Perivascular Space (DTI-ALPS) in Patients with Parkinson's Disease. *Oxid Med Cell Longev* 2021; **2021**: 4034509 [PMID: 33680283 DOI: 10.1155/2021/4034509]

17 **Shen T**, Yue Y, Ba F, He T, Tang X, Hu X, Pu J, Huang C, Lv W, Zhang B, Lai HY. Diffusion along perivascular spaces as marker for impairment of glymphatic system in Parkinson's disease. *NPJ Parkinsons Dis* 2022; **8**: 174 [PMID: 36543809 DOI: 10.1038/s41531-022-00437-1]

18 **Hsu JL**, Wei YC, Toh CH, Hsiao IT, Lin KJ, Yen TC, Liao MF, Ro LS. Magnetic Resonance Images Implicate That Glymphatic Alterations Mediate Cognitive Dysfunction in Alzheimer Disease. *Ann Neurol* 2023; **93**: 164-174 [PMID: 36214568 DOI: 10.1002/ana.26516]

19 **Yang G**, Deng N, Liu Y, Gu Y, Yao X. Evaluation of Glymphatic System Using Diffusion MR Technique in T2DM Cases. *Front Hum Neurosci* 2020; **14**: 300 [PMID: 32922272 DOI: 10.3389/fnhum.2020.00300]

20 **Tarasoff-Conway JM**, Carare RO, Osorio RS, Glodzik L, Butler T, Fieremans E, Axel L, Rusinek H, Nicholson C, Zlokovic BV, Frangione B, Blennow K, Ménard J, Zetterberg H, Wisniewski T, de Leon MJ. Clearance systems in the brain-implications for Alzheimer disease. *Nat Rev Neurol* 2015; **11**: 457-470 [PMID: 26195256 DOI: 10.1038/nrneurol.2015.119]

21 **Eide PK**, Ringstad G. MRI with intrathecal MRI gadolinium contrast medium administration: a possible method to assess glymphatic function in human brain. *Acta Radiol Open* 2015; **4**: 2058460115609635 [PMID: 26634147 DOI: 10.1177/2058460115609635]

22 **de Leon MJ**, Li Y, Okamura N, Tsui WH, Saint-Louis LA, Glodzik L, Osorio RS, Fortea J, Butler T, Pirraglia E, Fossati S, Kim HJ, Carare RO, Nedergaard M, Benveniste H, Rusinek H. Cerebrospinal Fluid Clearance in Alzheimer Disease Measured with Dynamic PET. *J Nucl Med* 2017; **58**: 1471-1476 [PMID: 28302766 DOI: 10.2967/jnumed.116.187211]

23 **Ota M**, Sato N, Nakaya M, Shigemoto Y, Kimura Y, Chiba E, Yokoi Y, Tsukamoto T, Matsuda H. Relationships Between the Deposition of Amyloid-β and Tau Protein and Glymphatic System Activity in Alzheimer's Disease: Diffusion Tensor Image Study. *J Alzheimers Dis* 2022; **90**: 295-303 [PMID: 36120782 DOI: 10.3233/JAD-220534]

24 **Bae YJ**, Kim JM, Choi BS, Choi JH, Ryoo N, Song YS, Cho SJ, Kim JH. Glymphatic function assessment in Parkinson's disease using diffusion tensor image analysis along the perivascular space. *Parkinsonism Relat Disord* 2023; **114**: 105767 [PMID: 37523953 DOI: 10.1016/j.parkreldis.2023.105767]

25 **Gu L**, Dai S, Guo T, Si X, Lv D, Wang Z, Lu J, Fang Y, Guan X, Zhou C, Wu H, Xu X, Yan Y, Song Z, Zhang MM, Zhang B, Pu J. Noninvasive neuroimaging provides evidence for deterioration of the glymphatic system in Parkinson's disease relative to essential tremor. *Parkinsonism Relat Disord* 2023; **107**: 105254 [PMID: 36584484 DOI: 10.1016/j.parkreldis.2022.105254]

26 **Qin Y**, He R, Chen J, Zhou X, Zhou X, Liu Z, Xu Q, Guo JF, Yan XX, Jiang N, Liao W, Taoka T, Wang D, Tang B. Neuroimaging uncovers distinct relationships of glymphatic dysfunction and motor symptoms in Parkinson's disease. *J Neurol* 2023; **270**: 2649-2658 [PMID: 36856846 DOI: 10.1007/s00415-023-11594-5]

27 **Bae YJ**, Kim JM, Choi BS, Ryoo N, Song YS, Nam Y, Yoon IY, Cho SJ, Kim JH. Altered Brain Glymphatic Flow at Diffusion-Tensor MRI in Rapid Eye Movement Sleep Behavior Disorder. *Radiology* 2023; **307**: e221848 [PMID: 37158722 DOI: 10.1148/radiol.221848]

28 **Zhao X**, Zhou Y, Li Y, Huang S, Zhu H, Zhou Z, Zhu S, Zhu W. The asymmetry of glymphatic system dysfunction in patients with temporal lobe epilepsy: A DTI-ALPS study. *J Neuroradiol* 2023; **50**: 562-567 [PMID: 37301366 DOI: 10.1016/j.neurad.2023.05.009]

29 **Bae YJ**, Choi BS, Kim JM, Choi JH, Cho SJ, Kim JH. Altered glymphatic system in idiopathic normal pressure hydrocephalus. *Parkinsonism Relat Disord* 2021; **82**: 56-60 [PMID: 33248394 DOI: 10.1016/j.parkreldis.2020.11.009]

30 **Page P**. Beyond statistical significance: clinical interpretation of rehabilitation research literature. *Int J Sports Phys Ther* 2014; **9**: 726-736 [PMID: 25328834]

31 **Mout L**, de Wit R, Stuurman D, Verhoef E, Mathijssen R, de Ridder C, Lolkema M, van Weerden W. Testosterone Diminishes Cabazitaxel Efficacy and Intratumoral Accumulation in a Prostate Cancer Xenograft Model. *EBioMedicine* 2018; **27**: 182-186 [PMID: 29276148 DOI: 10.1016/j.ebiom.2017.12.024]

32 **Liu X**, Barisano G, Shao X, Jann K, Ringman JM, Lu H, Arfanakis K, Caprihan A, DeCarli C, Gold BT, Maillard P, Satizabal CL, Fadaee E, Habes M, Stables L, Singh H, Fischl B, Kouwe AV, Schwab K, Helmer KG, Greenberg SM, Wang DJJ; MarkVCID Consortium. Cross-Vendor Test-Retest Validation of Diffusion Tensor Image Analysis along the Perivascular Space (DTI-ALPS) for Evaluating Glymphatic System Function. *Aging Dis* 2023 [PMID: 37307817 DOI: 10.14336/AD.2023.0321-2]

33 **McKnight CD**, Trujillo P, Lopez AM, Petersen K, Considine C, Lin YC, Yan Y, Kang H, Donahue MJ, Claassen DO. Diffusion along perivascular spaces reveals evidence supportive of glymphatic function impairment in Parkinson disease. *Parkinsonism Relat Disord* 2021; **89**: 98-104 [PMID: 34271425 DOI: 10.1016/j.parkreldis.2021.06.004]

34 **Arnold SE**, Arvanitakis Z, Macauley-Rambach SL, Koenig AM, Wang HY, Ahima RS, Craft S, Gandy S, Buettner C, Stoeckel LE, Holtzman DM, Nathan DM. Brain insulin resistance in type 2 diabetes and Alzheimer disease: concepts and conundrums. *Nat Rev Neurol* 2018; **14**: 168-181 [PMID: 29377010 DOI: 10.1038/nrneurol.2017.185]

35 **van Keulen K**, Knol W, Belitser SV, van der Linden PD, Heerdink ER, Egberts TCG, Slooter AJC. Diabetes and Glucose Dysregulation and Transition to Delirium in ICU Patients. *Crit Care Med* 2018; **46**: 1444-1449 [PMID: 29957712 DOI: 10.1097/CCM.0000000000003285]

36 **Durpès MC**, Morin C, Paquin-Veillet J, Beland R, Paré M, Guimond MO, Rekhter M, King GL, Geraldes P. PKC-β activation inhibits IL-18-binding protein causing endothelial dysfunction and diabetic atherosclerosis. *Cardiovasc Res* 2015; **106**: 303-313 [PMID: 25808972 DOI: 10.1093/cvr/cvv107]

37 **Kim OY**, Song J. The Role of Irisin in Alzheimer's Disease. *J Clin Med* 2018; **7** [PMID: 30388754 DOI: 10.3390/jcm7110407]

38 **Ye L**, Dai B, Wu Z, Hu Y. Dynamics of heart rate variability in patients with type 2 diabetes mellitus during spinal anesthesia using dexmedetomidine. *Am J Transl Res* 2021; **13**: 5395-5403 [PMID: 34150136]

39 **Wang YJ**, Sun YR, Pei YH, Ma HW, Mu YK, Qin LH, Yan JH. The lymphatic drainage systems in the brain: a novel target for ischemic stroke? *Neural Regen Res* 2023; **18**: 485-491 [PMID: 36018151 DOI: 10.4103/1673-5374.346484]

40 **Li W**, Chen D, Liu N, Luan Y, Zhu S, Wang H. Modulation of lymphatic transport in the central nervous system. *Theranostics* 2022; **12**: 1117-1131 [PMID: 35154477 DOI: 10.7150/thno.66026]

41 **Qin Y**, Li X, Qiao Y, Zou H, Qian Y, Li X, Zhu Y, Huo W, Wang L, Zhang M. DTI-ALPS: An MR biomarker for motor dysfunction in patients with subacute ischemic stroke. *Front Neurosci* 2023; **17**: 1132393 [PMID: 37065921 DOI: 10.3389/fnins.2023.1132393]

42 **Chormai P**, Pu Y, Hu H, Fisher SE, Francks C, Kong XZ. Machine learning of large-scale multimodal brain imaging data reveals neural correlates of hand preference. *Neuroimage* 2022; **262**: 119534 [PMID: 35931311 DOI: 10.1016/j.neuroimage.2022.119534]

43 **Samaras K**, Lutgers HL, Kochan NA, Crawford JD, Campbell LV, Wen W, Slavin MJ, Baune BT, Lipnicki DM, Brodaty H, Trollor JN, Sachdev PS. The impact of glucose disorders on cognition and brain volumes in the elderly: the Sydney Memory and Ageing Study. *Age*

(Dordr) 2014; **36**: 977-993 [PMID: 24402401 DOI: 10.1007/s11357-013-9613-0]

44 **Tuligenga RH**, Dugravot A, Tabák AG, Elbaz A, Brunner EJ, Kivimäki M, Singh-Manoux A. Midlife type 2 diabetes and poor glycaemic control as risk factors for cognitive decline in early old age: a post-hoc analysis of the Whitehall II cohort study. *Lancet Diabetes Endocrinol* 2014; **2**: 228-235 [PMID: 24622753 DOI: 10.1016/S2213-8587(13)70192-X]

45 **Chung CC**, Pimentel D, Jor'dan AJ, Hao Y, Milberg W, Novak V. Inflammation-associated declines in cerebral vasoreactivity and cognition in type 2 diabetes. *Neurology* 2015; **85**: 450-458 [PMID: 26156513 DOI: 10.1212/WNL.0000000000001820]

46 **Hsieh CF**, Liu CK, Lee CT, Yu LE, Wang JY. Acute glucose fluctuation impacts microglial activity, leading to inflammatory activation or self-degradation. *Sci Rep* 2019; **9**: 840 [PMID: 30696869 DOI: 10.1038/s41598-018-37215-0]

47 **Salameh TS**, Mortell WG, Logsdon AF, Butterfield DA, Banks WA. Disruption of the hippocampal and hypothalamic blood-brain barrier in a diet-induced obese model of type II diabetes: prevention and treatment by the mitochondrial carbonic anhydrase inhibitor, topiramate. *Fluids Barriers CNS* 2019; **16**: 1 [PMID: 30616618 DOI: 10.1186/s12987-018-0121-6]

48 **Mansouri S**, Barde S, Ortsäter H, Eweida M, Darsalia V, Langel U, Sjöholm A, Hökfelt T, Patrone C. GalR3 activation promotes adult neural stem cell survival in response to a diabetic milieu. *J Neurochem* 2013; **127**: 209-220 [PMID: 23927369 DOI: 10.1111/jnc.12396]

49 **Christman AL**, Matsushita K, Gottesman RF, Mosley T, Alonso A, Coresh J, Hill-Briggs F, Sharrett AR, Selvin E. Glycated haemoglobin and cognitive decline: the Atherosclerosis Risk in Communities (ARIC) study. *Diabetologia* 2011; **54**: 1645-1652 [PMID: 21360189 DOI: 10.1007/s00125-011-2095-7]

50 **Yaffe K**, Falvey CM, Hamilton N, Harris TB, Simonsick EM, Strotmeyer ES, Shorr RI, Metti A, Schwartz AV; Health ABC Study. Association between hypoglycemia and dementia in a biracial cohort of older adults with diabetes mellitus. *JAMA Intern Med* 2013; **173**: 1300-1306 [PMID: 23753199 DOI: 10.1001/jamainternmed.2013.6176]

51 **Wang J**, Zhou Y, Zhang K, Ran W, Zhu X, Zhong W, Chen Y, Li J, Sun J, Lou M. Glymphatic function plays a protective role in ageing-related cognitive decline. *Age Ageing* 2023; **52** [PMID: 37392401 DOI: 10.1093/ageing/afad107]

52 **Nigrovic LE**, Kimia AA, Shah SS, Neuman MI. Relationship between cerebrospinal fluid glucose and serum glucose. *N Engl J Med* 2012; **366**: 576-578 [PMID: 22316468 DOI: 10.1056/NEJMc1111080]

53 **Wu T**, Seaver P, Lemus H, Hollenbach K, Wang E, Pierce JP. Associations between Dietary Acid Load and Biomarkers of Inflammation and Hyperglycemia in Breast Cancer Survivors. *Nutrients* 2019; **11** [PMID: 31443226 DOI: 10.3390/nu11081913]

54 **Goedeke L**, Rotllan N, Canfrán-Duque A, Aranda JF, Ramírez CM, Araldi E, Lin CS, Anderson NN, Wagschal A, de Cabo R, Horton JD, Lasunción MA, Näär AM, Suárez Y, Fernández-Hernando C. MicroRNA-148a regulates LDL receptor and ABCA1 expression to control circulating lipoprotein levels. *Nat Med* 2015; **21**: 1280-1289 [PMID: 26437365 DOI: 10.1038/nm.3949]

55 **Inzucchi SE**, Viscoli CM, Young LH, Furie KL, Gorman M, Lovejoy AM, Dagogo-Jack S, Ismail-Beigi F, Korytkowski MT, Pratley RE, Schwartz GG, Kernan WN; IRIS Trial Investigators. Pioglitazone Prevents Diabetes in Patients With Insulin Resistance and Cerebrovascular Disease. *Diabetes Care* 2016; **39**: 1684-1692 [PMID: 27465265 DOI: 10.2337/dc16-0798]

56 **Iliodromiti S**, Celis-Morales CA, Lyall DM, Anderson J, Gray SR, Mackay DF, Nelson SM, Welsh P, Pell JP, Gill JMR, Sattar N. The impact of confounding on the associations of different adiposity measures with the incidence of cardiovascular disease: a cohort study of 296 535 adults of white European descent. *Eur Heart J* 2018; **39**: 1514-1520 [PMID: 29718151 DOI: 10.1093/eurheartj/ehy057]

57 **Myint PK**, Kwok CS, Luben RN, Wareham NJ, Khaw KT. Body fat percentage, body mass index and waist-to-hip ratio as predictors of mortality and cardiovascular disease. *Heart* 2014; **100**: 1613-1619 [PMID: 24966306 DOI: 10.1136/heartjnl-2014-305816]

58 **Kajani S**, Curley S, McGillicuddy FC. Unravelling HDL-Looking beyond the Cholesterol Surface to the Quality Within. *Int J Mol Sci* 2018; **19** [PMID: 29986413 DOI: 10.3390/ijms19071971]

59 **Fisher EA**, Feig JE, Hewing B, Hazen SL, Smith JD. High-density lipoprotein function, dysfunction, and reverse cholesterol transport. *Arterioscler Thromb Vasc Biol* 2012; **32**: 2813-2820 [PMID: 23152494 DOI: 10.1161/ATVBAHA.112.300133]

60 **Holy EW**, Besler C, Reiner MF, Camici GG, Manz J, Beer JH, Lüscher TF, Landmesser U, Tanner FC. High-density lipoprotein from patients with coronary heart disease loses anti-thrombotic effects on endothelial cells: impact on arterial thrombus formation. *Thromb Haemost* 2014; **112**: 1024-1035 [PMID: 25056722 DOI: 10.1160/TH13-09-0775]

61 **Kontush A**, Chapman MJ. Functionally defective high-density lipoprotein: a new therapeutic target at the crossroads of dyslipidemia, inflammation, and atherosclerosis. *Pharmacol Rev* 2006; **58**: 342-374 [PMID: 16968945 DOI: 10.1124/pr.58.3.1]

62 **Navab M**, Reddy ST, Van Lenten BJ, Fogelman AM. HDL and cardiovascular disease: atherogenic and atheroprotective mechanisms. *Nat Rev Cardiol* 2011; **8**: 222-232 [PMID: 21304474 DOI: 10.1038/nrcardio.2010.222]

63 **Sorrentino SA**, Besler C, Rohrer L, Meyer M, Heinrich K, Bahlmann FH, Mueller M, Horváth T, Doerries C, Heinemann M, Flemmer S, Markowski A, Manes C, Bahr MJ, Haller H, von Eckardstein A, Drexler H, Landmesser U. Endothelial-vasoprotective effects of high-density lipoprotein are impaired in patients with type 2 diabetes mellitus but are improved after extended-release niacin therapy. *Circulation* 2010; **121**: 110-122 [PMID: 20026785 DOI: 10.1161/CIRCULATIONAHA.108.836346]

64 **Taoka T**, Ito R, Nakamichi R, Kamagata K, Sakai M, Kawai H, Nakane T, Abe T, Ichikawa K, Kikuta J, Aoki S, Naganawa S. Reproducibility of diffusion tensor image analysis along the perivascular space (DTI-ALPS) for evaluating interstitial fluid diffusivity and glymphatic function: CHanges in Alps index on Multiple conditiON acquIsition eXperiment (CHAMONIX) study. *Jpn J Radiol* 2022; **40**: 147-158 [PMID: 34390452 DOI: 10.1007/s11604-021-01187-5]

Published by **Baishideng Publishing Group Inc**
7041 Koll Center Parkway, Suite 160, Pleasanton, CA 94566, USA
Telephone: +1-925-3991568
E-mail: office@baishideng.com
Help Desk: https://www.f6publishing.com/helpdesk
https://www.wjgnet.com